

Estimating Missing Observation of the Antarctic Ozone Hole

Bu Hyoung Lee and William W. S. Wei

Department of Statistics, Temple University, 1801 Liacouras Walk, Philadelphia, PA
19122

Abstract

The NASA has monitored the Antarctic ozone depletion referred to as the ozone hole, caused by manmade compounds, especially CFCs and BFCs, using satellite remote sensing instruments since the late 1970s. However, observations between December 1994 and June 1996 are missing because the NASA remote sensors were not in the observation orbit. We first construct nonlinear SETAR models for two sub-series from January 1983 to November 1994 and from July 1996 to December 2010. We then use the models to estimate the missing values using forward-forecasting, backward-forecasting, and the linear combination of forward-forecasts and backward forecasts.

Key Words: nonlinear time series, SETAR model, missing value estimation, forward-forecast, backward-forecast, forecasts-combining, ozone hole.

1. Introduction

Ozone (chemical formula: O_3), consisting of three oxygen atoms chemically bound, has big effects on people's health and the environment even though its amount is only 0.00006 percent of the atmosphere. The effects can be good or bad, depending on its location in the atmosphere. The tropospheric ozone existing in about 0 – 10 km altitude is an air-pollutant which is harmful to breathe. On the other hand, the stratospheric ozone residing in about 10 – 50 km altitude, known as the ozone layer, is a good shield which protects life on Earth from intense ultraviolet (UV) solar radiation (EPA; NASA, 2012; NOAA).

The first scientific research of ozone dates back to around 1840 when Christian F. Schönbein synthesized ozone in his laboratory. In the early twentieth century, the modern measurement of ozone was introduced by Fabry and Buisson (1913) and Dobson and Harrison (1926). A lot of new observations and discoveries of ozone over the past century help us understand the mechanism of ozone formation and destruction in the atmosphere. Especially, because of Molina and Rowland (1974)'s research on the chlorine-catalyzed ozone destruction and Farman, and Gardiner, and Shanklin (1985)'s report of large ozone reductions over Antarctica during spring of the Southern Hemisphere, it has been believed that man-made compounds such as chlorofluorocarbons (CFCs) and bromofluorocarbons (BFCs) are responsible for ozone depletion in the stratosphere (Solomon, 1999; Brönnimann et al, 2003; Rowland, 2006).

The National Aeronautics and Space Administration (NASA) has also monitored ozone values over the entire south polar region using satellite remote sensing instruments, such as the Total Ozone Mapping Spectrometer (TOMS) and the Ozone Monitoring

Instrument (OMI), over last 30 years and mapped the Antarctic ozone hole which is defined as the area with total ozone below 220 Dobson units, equivalent to pure ozone 2.2 millimeters thick at a temperature of 0 degrees Celsius and a pressure of 1 atmosphere. However, their satellite data from December 1994 to June 1996 are missing because the NASA program had no on-orbit capability during the 19 months (NASA, 2009).

Figure 1 displays the monthly average size of the Antarctic ozone hole between January 1983 and December 2010. It is clear that the ozone hole fluctuates seasonally; that is, the hole largely happens every spring from September through November, but it does not show up in other seasons. As shown in the figure, 19 observations between December 1994 and June 1996 are missing.

We first construct self-exciting threshold autoregressive (SETAR or TAR) nonlinear time series models for the two sub-series, one from January 1983 to November 1994 (143 months) and the other from July 1996 to December 2010 (174 months). We then use these models to estimate the 19 missing observations using forward-forecasting (forecasting), backward-forecasting (backcasting), and forecasts-combining.

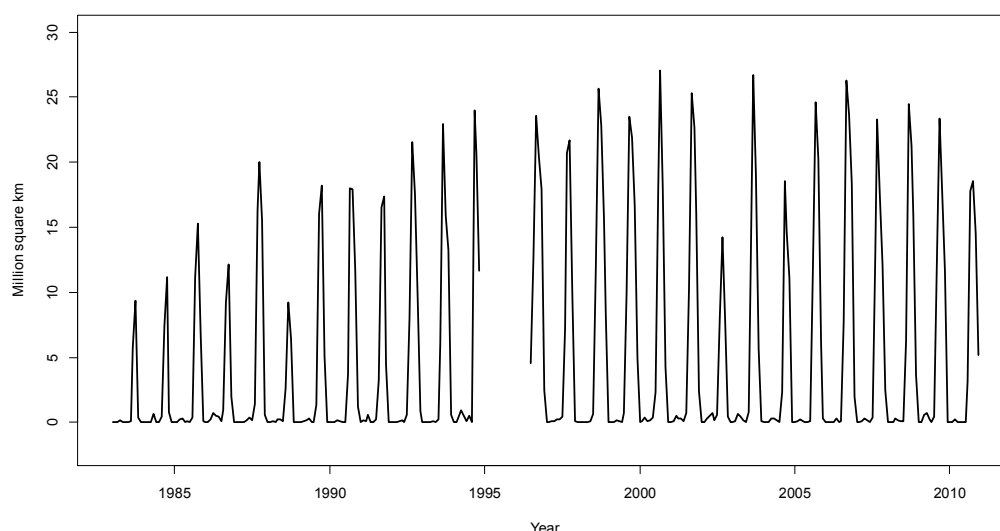


Figure 1: Monthly average size of the Antarctic ozone hole between 1983 and 2010.

2. Preliminary Study

We split the original ozone hole series (OZ) into two partial series such as $OZ1$ for the series with 143 observations from January 1983 to November 1994 and $OZ2$ for the series with 174 observations from July 1996 to December 2010. Let Z_t denote the original process of OZ , $Z_{1,t}$ be the first partial process of $OZ1$, and $Z_{2,t}$ be the second partial process of $OZ2$.

First, we investigate the sample ACFs and the sample PACFs of the series $OZ1$ and $OZ2$. As shown in Figure 2, strong seasonal variations with seasonal period 12 were detected in the both series. So we consider seasonal differencing of the two series; that is $W_{1,t} = (1 -$

$B^{12}Z_{1,t}$ denoting the seasonally differenced series of OZ1, say OZ1.s12, and $W_{2,t} = (1 - B^{12})Z_{2,t}$ denoting the seasonally differenced series of OZ2, say OZ2.s12.

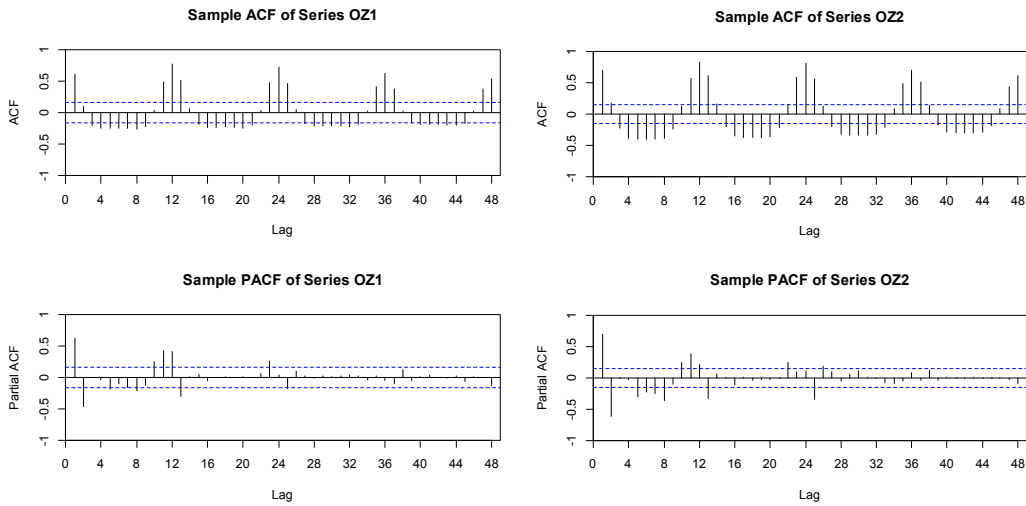


Figure 2: Sample ACF and sample PACF of series OZ1 (left) and OZ2 (right).

3. Model Building: Nonlinear SETAR Models

We now employ the likelihood ratio test for threshold nonlinearity (Chan, 1991) and the arranged autoregression approach (Tsay, 1989; Tsay, 2010; Wei, 2006) to construct self-exciting TAR models (Tong and Lim, 1980) for series OZ1 and series OZ2.

3.1. Model Identification

Step 1. Tentatively select the AR order.

First, we select the maximum AR orders to be entertained for the two piecewise linear AR models. Here, we tentatively choose the AR order $P_1 = 13$ for series OZ1.s12 and $P_2 = 13$ for series OZ2.s12 because their AIC values are minimum in Table 1.

Table 1: The AIC values of the two linear AR(p) models of OZ1.s12 and OZ2.s12.

Series	$p = 0$	1	2	3	4	5	6	7
OZ1.s12	74.1	35.5	36.5	37.9	39.8	41.8	43.8	45.8
OZ2.s12	147.8	96.5	89.3	89.8	87.6	88.2	90.2	91.8
Series	$p = 8$	9	10	11	12	13	14	15
OZ1.s12	47.8	49.6	46.1	28.1	8.3	0.0	1.5	3.2
OZ2.s12	93.7	95.4	71.1	59.0	29.1	0.0	2.0	3.0

Step 2. Searching for the delay parameter d and hence the threshold variables

$W_{i,t-d}$, $i = 1, 2$.

Let $D_i = \{1, 2, \dots, P_i\}$ be the set of possible delay lag of $W_{i,t-d}$, $i = 1, 2$. Then we fit the arranged autoregressions for the given P_i and every element d_i of D_i , and perform the likelihood ratio test for threshold nonlinearity. The results of the threshold nonlinearity

tests are summarized in Table 2. We choose $d_1 = 11$ and $d_2 = 7$ because they produce the largest test statistics and the smallest p -values respectively. Thus, $W_{1,t-11}$ and $W_{2,t-7}$ are the threshold variables of series OZ1.s12 and OZ2.s12, respectively.

Table 2: The summary of the threshold nonlinearity test of OZ1.s12 and OZ2.s12.

Series	d	Test statistic	p -value	Series	d	Test statistic	p -value
OZ1.s12	1	33.72435	0.03467	OZ2.s12	1	24.34353	0.24539
	2	28.28114	0.12637		2	23.62481	0.26913
	3	39.27506	0.00701		3	24.90071	0.22681
	4	36.36273	0.01667		4	28.77328	0.11281
	5	33.32534	0.03853		5	34.96831	0.02442
	6	34.41601	0.02877		6	32.71728	0.04460
	7	44.14823	0.00148		7	46.43210	0.00068
	8	31.93437	0.05503		8	27.83821	0.13651
	9	33.27651	0.03903		9	18.91528	0.35877
	10	28.34929	0.12462		10	36.12061	0.01765
	11	49.36983	0.00025		11	26.37419	0.17909
	12	22.99352	0.29224		12	41.39531	0.00357
	13	23.84785	0.26459		13	35.77265	0.01949

Step 3. Search for the threshold values.

To search for the threshold values, we construct a scatterplot of the t -ratios of $\hat{\phi}_{1,11}$, which denotes the recursive estimate of the lag-11 AR parameter in the arranged autoregression of series OZ1.s12, versus the ordered values $W_{1,t-11}$ in the left panel of Figure 3. Similarly, the scatterplot of the t -ratios of $\hat{\phi}_{2,7}$, which denotes the recursive estimate of the lag-7 AR parameter in the arranged autoregression of series OZ2.s12, versus the ordered values $W_{2,t-7}$ is shown in the right panel of Figure 3. From the left plot, we see the t -ratio has a big drop and then an increase at $W_{1,t-11} = 0.6$, suggesting that we have a two-regime model with the threshold value $r_1 = 0.6$, i.e., a TAR(2; $p_{1,1}, p_{1,2}; 11$) model for series OZ1.s12. Similarly, in the right plot, the t -ratio has a big drop and then a convex-upward increase at $W_{2,t-7} = -0.07$, indicating a two-regime model with the threshold value $r_2 = -0.07$, i.e., a TAR(2; $p_{2,1}, p_{2,2}; 7$) model for series OZ2.s12.

Step 4. Finally select the self-exciting threshold AR order

We compare the AIC values of all possible models, TAR(2; $p_{1,1}, p_{1,2}; 11$) models for series OZ1.s12 and TAR(2; $p_{2,1}, p_{2,2}; 7$) models for series OZ2.s12, using `setar` function of `tsDyn` package in R and then find the AR order in each regime based on the minimum AIC value. The results lead to a TAR(2; 13, 11; 11) model for series OZ1.s12 since the minimum AIC value is 215.233 when $p_{1,1} = 13$ and $p_{1,2} = 11$, and a TAR(2; 13, 13; 7) model for series OZ2.s12 since the minimum AIC value is 281.590 when $p_{1,1} = 13$ and $p_{2,2} = 13$.

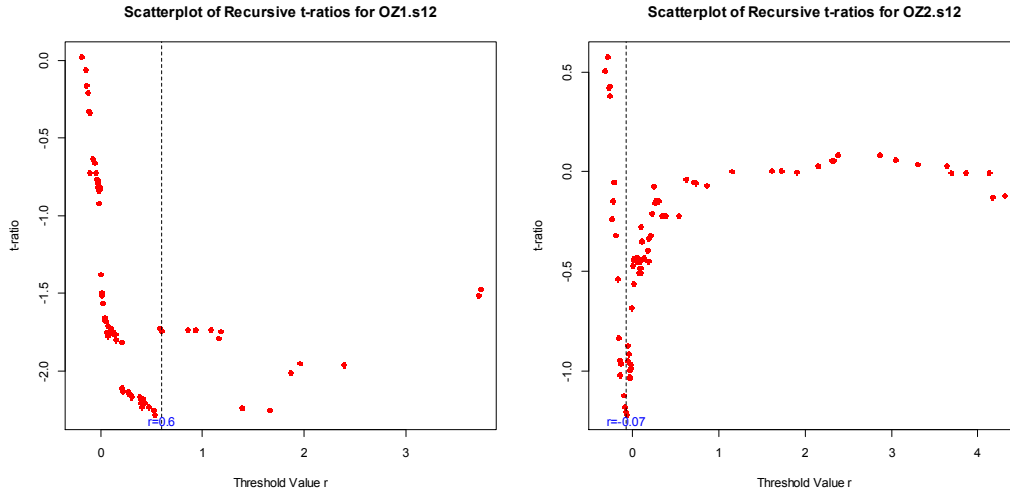


Figure 3: Scatterplot (left) of recursive t -ratios of the lag-11 AR coefficient $\hat{\phi}_{1,11}$ versus ordered $W_{1,t-11}$ and scatterplot (right) of recursive t -ratios of the lag-7 AR coefficient $\hat{\phi}_{2,7}$ versus ordered $W_{2,t-7}$.

3.2. Parameter Estimation

Now, we estimate parameter coefficients of the differenced series, $W_{i,t} = (1 - B^{12})Z_{i,t}$, $i = 1, 2$, for each model. The fitted model of the TAR(2; 13, 11; 11) is written as the forward form:

$$\begin{aligned}
 W_{1,t} = & \underset{(0.234)}{0.287} + \underset{(0.104)}{0.300}W_{1,t-1} + \underset{(0.088)}{0.019}W_{1,t-2} - \underset{(0.085)}{0.008}W_{1,t-3} - \underset{(0.085)}{0.022}W_{1,t-4} + \underset{(0.083)}{0.010}W_{1,t-5} \\
 & - \underset{(0.083)}{0.025}W_{1,t-6} + \underset{(0.084)}{0.010}W_{1,t-7} + \underset{(0.087)}{0.004}W_{1,t-8} - \underset{(0.099)}{0.048}W_{1,t-9} + \underset{(0.111)}{0.056}W_{1,t-10} \\
 & - \underset{(0.108)}{0.186}W_{1,t-11} - \underset{(0.123)}{0.611}W_{1,t-12} + \underset{(0.113)}{0.285}W_{1,t-13} + a_t^{(1)}, \\
 & \text{if } W_{1,t-11} < 0.6,
 \end{aligned}$$

$$\begin{aligned}
 W_{1,t} = & \underset{(0.700)}{0.564} + \underset{(0.165)}{0.401}W_{1,t-1} + \underset{(0.362)}{1.667}W_{1,t-2} + \underset{(0.328)}{0.575}W_{1,t-3} - \underset{(1.058)}{1.358}W_{1,t-4} + \underset{(2.142)}{0.078}W_{1,t-5} \\
 & + \underset{(3.283)}{1.442}W_{1,t-6} - \underset{(1.930)}{2.572}W_{1,t-7} + \underset{(1.967)}{0.888}W_{1,t-8} + \underset{(0.245)}{0.220}W_{1,t-9} + \underset{(0.159)}{0.067}W_{1,t-10} \\
 & - \underset{(0.129)}{0.669}W_{1,t-11} + a_t^{(2)}, \\
 & \text{if } W_{1,t-11} \geq 0.6,
 \end{aligned}$$

where the values in parentheses below the parameter estimates are the associated standard errors and $a_t^{(j)}$, $j = 1, 2$, is a white noise series with mean zero and a constant variance. The numbers of observations are 95 and 23, and the residual variances are 3.067 and 7.597, respectively.

Similarly, we fit the TAR(2; 13, 13; 7) model and express it as the backward form:

$$\begin{aligned}
 W_{2,t} = & \underset{(0.401)}{0.260} + \underset{(0.122)}{1.021}W_{2,t+1} - \underset{(0.146)}{0.446}W_{2,t+2} + \underset{(0.148)}{0.193}W_{2,t+3} + \underset{(0.124)}{0.026}W_{2,t+4} - \underset{(0.145)}{0.024}W_{2,t+5} \\
 & + \underset{(0.134)}{0.093}W_{2,t+6} - \underset{(0.113)}{0.076}W_{2,t+7} + \underset{(0.116)}{0.017}W_{2,t+8} + \underset{(0.107)}{0.100}W_{2,t+9} - \underset{(0.111)}{0.301}W_{2,t+10} \\
 & + \underset{(0.153)}{0.217}W_{2,t+11} - \underset{(0.150)}{0.832}W_{2,t+12} + \underset{(0.119)}{0.531}W_{2,t+13} + e_t^{(1)},
 \end{aligned}$$

if $W_{1,t+7} < -0.07$,

$$\begin{aligned}
 W_{2,t} = & \underset{(0.265)}{0.098} + \underset{(0.105)}{0.411}W_{2,t+1} - \underset{(0.085)}{0.019}W_{2,t+2} - \underset{(0.087)}{0.036}W_{2,t+3} + \underset{(0.093)}{0.080}W_{2,t+4} - \underset{(0.092)}{0.050}W_{2,t+5} \\
 & + \underset{(0.093)}{0.009}W_{2,t+6} + \underset{(0.102)}{0.019}W_{2,t+7} - \underset{(0.113)}{0.058}W_{2,t+8} + \underset{(0.106)}{0.071}W_{2,t+9} - \underset{(0.101)}{0.088}W_{2,t+10} \\
 & + \underset{(0.088)}{0.013}W_{2,t+11} - \underset{(0.088)}{0.673}W_{2,t+12} + \underset{(0.106)}{0.384}W_{2,t+13} + e_t^{(2)},
 \end{aligned}$$

if $W_{1,t+7} \geq -0.07$,

where the values in parentheses below the parameter estimates are the associated standard errors and $e_t^{(j)}$, $j = 1, 2$, is a white noise series with mean zero and a constant variance. The numbers of observations are 58 and 91, and the residual variances are 4.647 and 4.302 respectively.

3.3. Diagnostic Checking

We draw the diagnostic residual plots of the TAR(2; 13, 11; 11) model and the TAR(2; 13, 13; 7) model, which are displayed in Figure 4. The residual ACFs of the two models show no significant peaks except at lag-0, and the Ljung-Box statistics are not significant at $\alpha = 0.05$. So the diagnostic plots do not show any evidence that the residuals are not white noise. In other words, the TAR(2; 13, 13; 11) model for series OZ1.s12 and the TAR(2; 13, 13; 7) model for series OZ2.s12 are adequate.

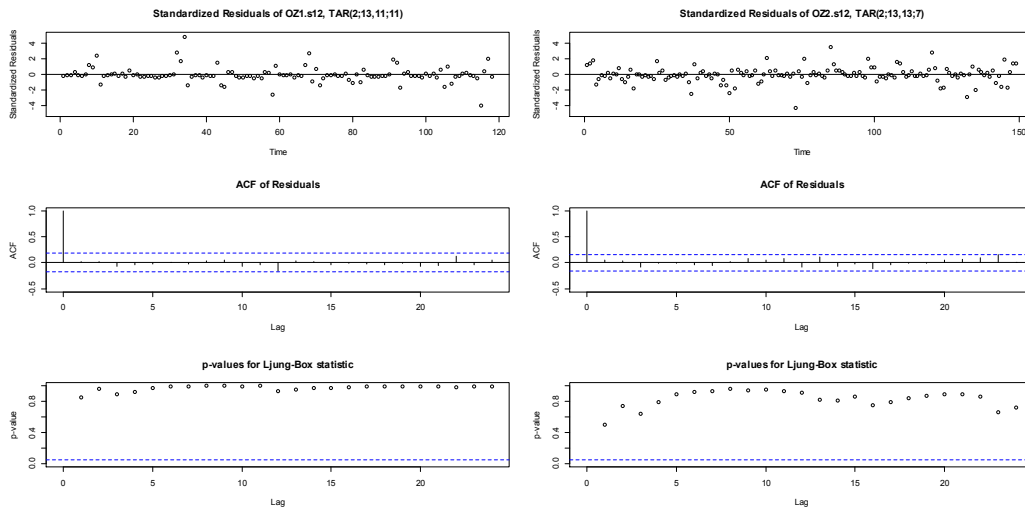


Figure 4: Diagnostic residual plots (left) for the TAR(2; 13, 11; 11) model and diagnostic residual plots (right) for the TAR(2; 13, 13; 7) model.

We also draw the fitted line of the forward form of the TAR(2; 13, 11; 11) model, the backward form of the TAR(2; 13, 13; 7) model, and their 95% confidence limits in Figure 5. The models fit quite well as most observations of the ozone hole series lie in the 95% confidence limits.

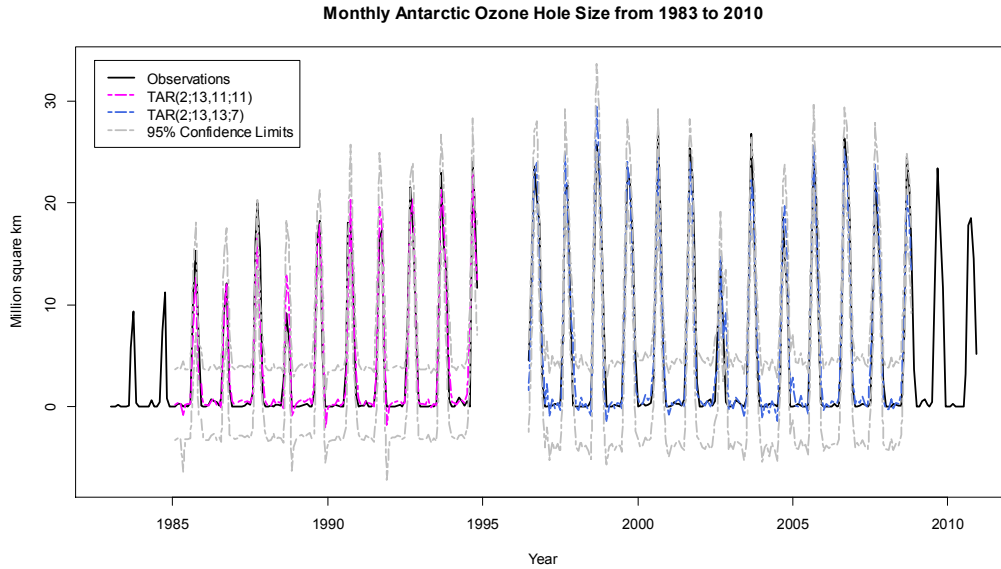


Figure 5: The fitted values for the TAR(2; 13, 11; 11) model, the TAR(2; 13, 13; 7) model, and their 95% confidence limits.

4. Estimating Missing Observations

4.1 Estimating the Missing Observations Using the TAR Models

We now estimate the missing 19 observations from December 1994 to June 1996 using forward-forecasting from the TAR(2; 13, 11; 11) model of series OZ1.s12. These 19 forward-forecasts for $W_{1,144} = W_{144}, \dots, W_{1,162} = W_{162}$, are as follows:

$$\begin{aligned} \hat{W}_{1,143}(1) &= 0.287 + 0.300W_{1,143} + 0.019W_{1,142} - 0.008W_{1,141} - 0.022W_{1,140} + 0.010W_{1,139} \\ &\quad - 0.025W_{1,138} + 0.010W_{1,137} + 0.004W_{1,136} - 0.048W_{1,135} + 0.056W_{1,134} \\ &\quad - 0.186W_{1,133} - 0.611W_{1,132} + 0.285W_{1,131} = 1.21, \end{aligned}$$

since $W_{1,133} = 0.00 < 0.6$,

⋮

$$\begin{aligned} \hat{W}_{1,143}(19) &= 0.564 + 0.401\hat{W}_{1,143}(18) + 1.667\hat{W}_{1,143}(17) + 0.575\hat{W}_{1,143}(16) - 1.358\hat{W}_{1,143}(15) \\ &\quad + 0.078\hat{W}_{1,143}(14) + 1.442\hat{W}_{1,143}(13) - 2.572\hat{W}_{1,143}(12) + 0.888\hat{W}_{1,143}(11) \\ &\quad + 0.220\hat{W}_{1,143}(10) + 0.067\hat{W}_{1,143}(9) - 0.669\hat{W}_{1,143}(8) = 0.36, \end{aligned}$$

since $\hat{W}_{1,143}(18) = 1.10 \geq 0.6$,

Next, we estimate the missing 19 observations from December 1994 to June 1996 using backward-forecasting from the TAR(2; 13, 13; 7) model. These 19 backward-forecasts for $W_{2,-1} = W_{162}, \dots, W_{2,-19} = W_{144}$, are computed as follows:

$$\begin{aligned}\hat{W}_{2,1}(-1) &= 0.098 + 0.411W_{2,1} - 0.019W_{2,2} - 0.036W_{2,3} + 0.080W_{2,4} - 0.050W_{2,5} \\ &\quad + 0.009W_{2,6} + 0.019W_{2,7} - 0.058W_{2,8} + 0.071W_{2,9} - 0.088W_{2,10} \\ &\quad + 0.013W_{2,11} - 0.673W_{2,12} + 0.384W_{2,13} = 0.94,\end{aligned}$$

since $W_{2,7} = 0.00 \geq -0.07$,

⋮

$$\begin{aligned}\hat{W}_{2,1}(-19) &= 0.260 + 1.021\hat{W}_{2,1}(-18) - 0.446\hat{W}_{2,1}(-17) + 0.193\hat{W}_{2,1}(-16) + 0.026\hat{W}_{2,1}(-15) \\ &\quad - 0.024\hat{W}_{2,1}(-14) + 0.093\hat{W}_{2,1}(-13) - 0.076\hat{W}_{2,1}(-12) + 0.017\hat{W}_{2,1}(-11) \\ &\quad + 0.100\hat{W}_{2,1}(-10) - 0.301\hat{W}_{2,1}(-9) + 0.217\hat{W}_{2,1}(-8) - 0.832\hat{W}_{2,1}(-7) \\ &\quad + 0.531\hat{W}_{2,1}(-6) = 1.80,\end{aligned}$$

since $\hat{W}_{2,1}(-12) = -2.25 < -0.07$,

4.2. Combinations of the forward-forecasts and the backward-forecasts

Since a linear combination of two estimations outperforms either of them (Granger and Ramanathan, 1984), we combine the forward-forecasts and the backward-forecast to obtain third estimations for these missing values using the weighted average technique of Bates and Granger (1969).

Let $F_{T_1}(i)$ be an unbiased i step forward-forecast at time T_1 and $B_{T_2}(j)$ be an unbiased j step backward-forecast at time T_2 where $T_2 - T_1 = i + j - 1$. The combined forecast $C(T_1 + i)$ at time $T_1 + i$ or $C(T_2 - j)$ at time $T_2 - j$ is given by

$$C(T_1 + i) = C(T_2 - j) = (1 - k)F_{T_1}(i) + kB_{T_2}(j)$$

where the optimal weight $k = \sigma_F^2 / (\sigma_F^2 + \sigma_B^2)$ with the forward-forecast variance σ_F^2 and the backward-forecast variance σ_B^2 assuming the forward-forecast error and the backward-forecast error are not correlated. The residual variances of the forward model and the backward model can be used instead of σ_F^2 and σ_B^2 (Balakrishnan, 2010).

Here we convert the estimations of $W_{i,t}$ to the estimations of $Z_{i,t}$ using the relation $\hat{W}_{i,t} = (1 - B^{12})\hat{Z}_{i,t}$, or equivalently, $\hat{Z}_{i,t} = \hat{W}_{i,t} - \hat{Z}_{i,t-12}$, $i = 1, 2$. Then we apply the combination method to 19 forward-forecasts of series OZ1 and 19 backward-forecasts of series OZ2. We remark that there are four optimal weights because of two sub-models in the forward model and two sub-models in the backward model.

Table 3, Figure 6, and Figure 7 present the three types of estimations—forward-forecasts, backward-forecasts, and their combinations for the 19 missing observations of the monthly series of the Antarctic ozone hole size between 1983 and 2010.

Table 3: Estimations of the 19 missing observations for the ozone hole series, between December 1994 and June 1996.

<i>Date</i>	<i>Forecasts</i>	<i>Backcasts</i>	<i>Combinations</i>
Dec.1994	1.83	2.75	2.20
Jan.1995	0.41	1.43	0.82
Feb.1995	0.50	0.24	0.40
Mar.1995	0.44	0.82	0.68
Apr.1995	-0.87	1.38	0.02
May.1995	0.64	1.77	1.09
Jun.1995	0.00	1.75	0.69
Jul.1995	1.63	2.32	1.92
Aug.1995	4.61	9.50	7.73
Sep.1995	24.09	21.87	22.67
Oct.1995	28.57	22.27	25.95
Nov.1995	16.38	12.81	14.10
Dec.1995	9.24	0.96	5.79
Jan.1996	3.06	-0.52	1.57
Feb.1996	1.12	0.47	0.85
Mar.1996	1.39	0.09	0.87
Apr.1996	0.44	0.60	0.51
May.1996	0.60	0.75	0.66
Jun.1996	0.36	1.18	0.89

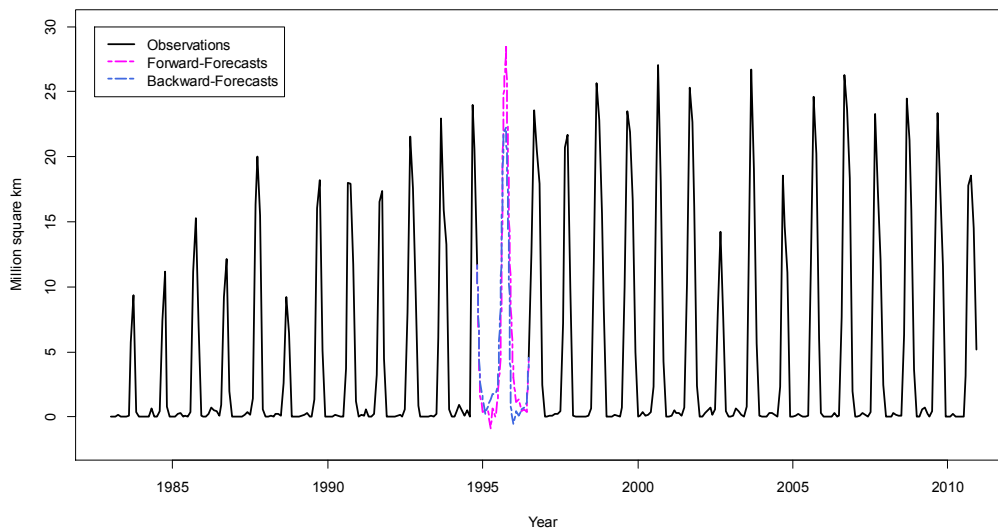


Figure 6: Monthly observations and estimations of the missing values from forward-forecasts and backward-forecasts of the Antarctic ozone hole series between 1983 and 2010.

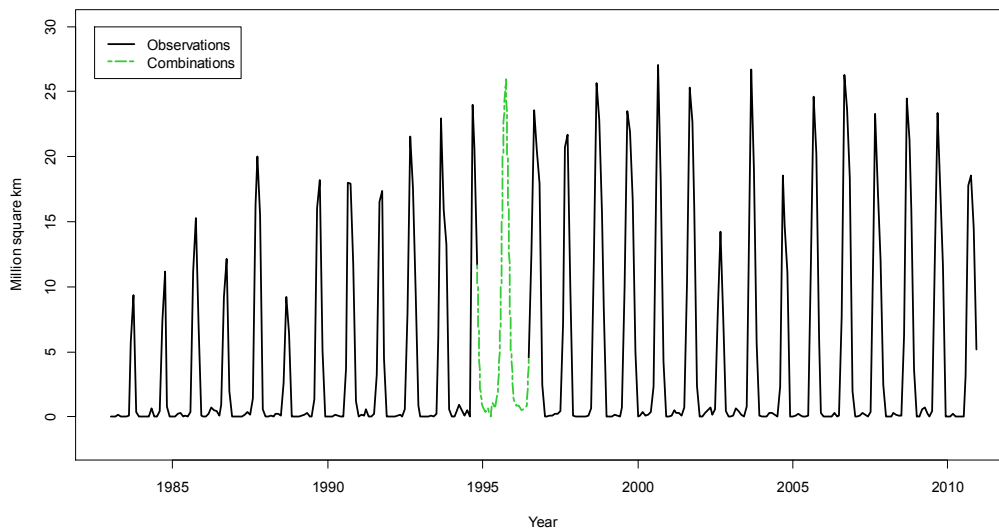


Figure 7: Monthly observations and the combining estimation of the missing values of the Antarctic ozone hole series between 1983 and 2010.

From Table 3, Figure 6, and Figure 7, we see that the forward-forecasts and the backward-forecasts produce similar stochastic trends even though the forward-forecasts estimate a larger ozone hole in spring of 1995. We also notice that they produce negative hole sizes in April 1995 and January 1996, respectively. However, the negative estimations disappear when linear combinations of the forward-forecasts and the backward-forecasts are used.

5. Conclusion

In this research, we estimated the 19 missing observations of the Antarctic ozone hole size series between December 1994 and June 1996 using the SETAR modeling of the two available sub-series. As shown above, the forward-forecasts and the backward-forecasts show similar stochastic trends, in general.

The combinations make the forecasts moderate; for example, the estimated large hole size from the forward-forecast in spring 1995 have been moderated when the combining method is used. Also, estimated negative hole sizes, from the forward-forecast in April 1995 and the backward-forecast in January 1996, disappear through the use of combining forecasts. The results suggest that the linear combination of forecasts provides good estimations for the missing observations of the Antarctic ozone hole size series.

References

- Balakrishnan, N. (2010), *Methods and Applications of Statistics in Business, Finance, and Management Science*, Hoboken, NJ: John Wiley & Sons.
- Bates, J. M., and Granger, C. W. J. (1969), "The combination of forecasts," *Operations Research Quarterly*, 20, 451–468.
- Brönnimann, S., Staehelin, J., Farmer, S. F. G., Cain, J. C., Svendby, T., and Svenøe T. (2003), "Total ozone observations prior to the IGY. I: A history," *Quarterly Journal of the Royal Meteorological Society*, 129, 2797–2817.
- Chan, K. S. (1991), "Percentage points of likelihood ratio tests for threshold autoregression," *Journal of the Royal Statistical Society, Series B*, 53, 691–696.
- Dobson, G. M. B., and Harrison, D. N. (1926), "Observations of the amount of ozone in the Earth's atmosphere and its relation to other geophysical conditions," *Proceedings of the Royal Society of London, Series A*, 110, 660–693.
- Fabry, C., and Buisson, H. (1913), "L'absorption de l'ultraviolet par l'ozone et la limite du spectre solaire," *Journal de Physique, Série 5*, 3, 196–206.
- Farman, J. C., Gardiner, B. G., and Shanklin, J. D. (1985), "Large losses of ozone in Antarctica reveal seasonal ClO_x/NO_x interaction," *Nature*, 315, 207–210.
- Granger, C. W. J., and Ramanathan, R., (1984). "Improved methods of combining forecasts," *Journal of Forecasting*, 3, 197–204.
- Molina, M. J., and Rowland, F. S. (1974), "Chlorine atomcatalysed destruction of ozone," *Nature*, 249, 810–812.
- Rowland, F. S. (2006), "Stratospheric ozone depletion," *Philosophical Transactions Royal Society B*, 361, 769–790.
- Solomon, S. (1999), "Stratospheric ozone depletion: A review of concepts and history," *Reviews of Geophysics*, 37, 275–316.
- Tong, H., and Lim, K. S. (1980), "Threshold autoregression, limit cycles and cyclical data (with discussion)," *Journal of the Royal Statistical Society, Series B*, 42, 245–292.
- Tsay, R. S. (1989), "Testing and modeling threshold autoregressive processes," *Journal of the American Statistical Association*, 84, 231–240.
- Tsay, R. S. (2010), *Analysis of Financial Time Series* (3rd ed.), Hoboken, NJ: John Wiley & Sons.
- Wei, W. W. S. (2006), *Time Series Analysis: Univariate and Multivariate Methods* (2nd ed.), Boston, MA: Addison Wesley.
- National Aeronautics and Space Administration (NASA) Goddard Space Flight Center. 2009, September 28. *The Missions of the Total Ozone Mapping Spectrometer*. Retrieved from <http://toms.gsfc.nasa.gov/fltmodel/spacecr.html>
- National Aeronautics and Space Administration (NASA) Goddard Space Flight Center. 2012, May 3. *Ozone Hole Watch: Images, data, and information for the Southern Hemisphere*. Retrieved from <http://ozonewatch.gsfc.nasa.gov/SH.htm>
- National Oceanic and Atmospheric Administration (NOAA). 2008, March 20. *The Science of Stratospheric Ozone*. Retrieved from <http://www.ozonelayer.noaa.gov/science/science.htm>
- United States Environmental Protection Agency (EPA). 2010, August 19. *Ozone Science: The facts behind the phaseout*. Retrieved from http://www.epa.gov/ozone/science/sc_fact.html